Available online at www.sciencedirect.com
ScienceDirect
Physica B 403 (2008) 184–189
PHYSICA B
www.elsevier.com/locate/physb

Photoluminescence and Raman spectra of the ordered vacancy compound $CuGa_5Se_8$

M. Grossberg[a,*], J. Krustok[a], I. Bodnar[b], S. Siebentritt[c], J. Albert[d]

[a]*Tallinn University of Technology, Ehitajate tee 5, 19086 Tallinn, Estonia*
[b]*Department of Chemistry, Belarussian State University of Informatics and Radioelectronics, P. Brovka str. 6, 220027 Minsk, Belarus*
[c]*Université du Luxembourg, 162a avenue de la Faïencerie, L-1511, Luxembourg*
[d]*Hahn-Meitner Institut, Glienicker Straße 100, 14109 Berlin, Germany*

Received 10 July 2007; received in revised form 16 August 2007; accepted 22 August 2007

Abstract

We studied the photoluminescence (PL) and Raman properties of the ordered defect compound $CuGa_5Se_8$. Twelve peaks were detected from the room-temperature Raman spectra with the A_1 mode around 160 cm^{-1}. Due to the stress in the polycrystalline thin film the corresponding frequencies of the Raman modes of a $CuGa_5Se_8$ single crystal were slightly shifted. One broad asymmetric PL band at 1.788 and 1.765 eV was observed at 10 K in the PL spectra of $CuGa_5Se_8$ single crystal and polycrystalline layer, respectively. The temperature and laser power dependencies of the PL spectra were also studied. The shape and properties of the PL band assure the presence of potential fluctuations and the analyses of the PL data suggest that the emission is due to band-to-tail (BT) or band-to-impurity (BI) recombination.
© 2007 Elsevier B.V. All rights reserved.

PACS: 71.20.Nr; 78.55.−M; 78.30.−J

Keywords: $CuGa_5Se_8$; Chalcopyrite crystals; Raman spectroscopy; Photoluminescence; Ordered defect compounds; Potential fluctuations

1. Introduction

One of the reasons why ternary chalcopyrite compounds are interesting is their toleration of a large range of anion to cation off-stoichiometry that leads to the existence of a number of ordered defect compounds [1]. It is reported that solar cells with the efficiency around 19% have been produced [2] using thin films based on $CuIn(Ga)Se_2$. The ordered defect compound $CuIn_3Se_5$ that precipitates as a secondary phase on the thin film surface of In-rich $CuInSe_2$ [3] is expected to improve the efficiency of such cells. Apart form $CuIn_3Se_5$, other In-rich phases like $CuIn_5Se_8$ and Ga-rich phases $CuGa_3Se_5$ and $CuGa_5Se_8$ have been reported [4,5] in the Cu_2Se–In_2Se_3 and Cu_2Se–Ga_2Se_3 quasi-binary systems, respectively. These compounds are called ordered vacancy compunds (OVCs), because vacancies are expected to orderly occupy particular crystallographic sites in their crystal structure to satisfy the four electrons per site rule [6]. They are also referred to as ordered defect compounds (ODCs) since Zhang et al. [1] have explained the existence and stability of these compounds with the presence of $(In_{Cu}^{2+} + 2V_{Cu}^{-1})$ donor–acceptor defect pairs (DADPs) that have very low formation energies.

In this paper we present the results of Raman and photoluminescence studies of $CuGa_5Se_8$. To our knowledge, very little work on the physical properties of $CuGa_5Se_8$ appear in the literature and there are no photoluminescence studies of $CuGa_5Se_8$ published. The temperature dependence of the energy gap in bulk samples of $CuGa_5Se_8$ have been reported by Marin et al. [5]. It was found that the bandgap energy varies from 1.917 to 1.811 eV in the temperature range between 10 and 300 K. Xu et al. [7] have investigated Raman spectra of $Cu(In_{1-x}Ga_x)_5Se_8$ thin films with varying x. To our knowledge, this is the only Raman spectrum of $CuGa_5Se_8$

*Corresponding author. Tel.: +372 6203210; fax: +372 6203367.
E-mail address: mgross@staff.ttu.ee (M. Grossberg).

0921-4526/$ - see front matter © 2007 Elsevier B.V. All rights reserved.
doi:10.1016/j.physb.2007.08.098

in the literature. From room-temperature Raman measurements they found seven peaks at 78, 93, 107, 160, 259 and 289 cm^{-1}, the peak at 160 cm^{-1} being the dominant A_1 mode of $CuGa_5Se_8$. However, no fitting of the spectra have been performed and no more detailed identification or assignment of the observed peaks has been made. Orlova et al. [8,9] have investigated the structural parameters, the axial thermal expansion coefficients and the characteristic Debye temperature of the $CuGa_5Se_8$ single crystals by using X-ray diffraction method. The unit cell parameters $a = 0.54682$ nm and $c = 1.09116$ nm were determined. It was also found that $CuGa_5Se_8$ has very close to $CuGa_3Se_5$ value of thermal expansion coefficient. There is also only a small difference in the crystal lattice parameters of these compounds. These properties of OVC compounds are essential for obtaining the high-quality epitaxial layers, for forming heterojunctions and for producing solar cells based on these ternary compounds. Leon et al. [10] have studied $CuGa_5Se_8$ by spectroscopic ellipsometry and determined the dielectric-function-related optical constants, such as the complex refractive index, extinction coefficient, absorption coefficient and normal-incidence reflectivity.

In order to understand the role of the ordered vacancies, we studied the photoluminescence and Raman spectra of $CuGa_5Se_8$ polycrystalline thin films and single crystals. To identify the observed Raman modes, the data obtained are compared with Raman spectra of $CuGa_5Se_8$ thin films reported in the literature [7].

2. Experimental methods

The MOCVD grown $CuGa_5Se_8$ polycrystalline thin films and single crystals grown by the vertical Bridgman method used in the present study exhibit compositions very close to its ideal value of 1:5:8 as measured by energy dispersive X-ray spectroscopy (EDX). The $CuGa_5Se_8$ thin films are grown in an Aixtron AIX200 MOCVD reactor on GaAs substrates. Cyclopentadienyl–copper, triethyl–gallium and ditertiary-butyl–selenide were used as Cu-, Ga- and Se-precursor, respectively. The growth process was derived from the process for $CuGaSe_2$ [11]. The growth temperature 570 °C was used and the reactor pressure was kept at 50 mbar. The processing time was 4 h. The dependence of the composition ratio on the partial pressure ratio was not linear. From the SEM images the polycrystallinity of the films was detected. The $CuGa_5Se_8$ single crystals were grown by the horizontal Bridgman method. The directed crystallization of the melt was performed by cooling of the furnace of the hot-zone up to ~1170 K at a rate of ~2 K h^{-1}. For more growth details of see Ref. [9].

The photoluminescence and room-temperature Raman spectra were recorded by using a Horiba's LabRam HR high resolution spectrometer equipped with a multichannel detection system in the backscattering configuration. In micro-Raman measurements, the incident laser light with the wavelength of 532 nm can be focused on the sample within a spot of 1 μm in diameter and the spectral resolution of the spectrometer is about 0.5 cm^{-1}. For photoluminescence measurements, the samples were mounted in the closed-cycle He cryostat and cooled down to 10 K. The 441.6 nm He–Cd laser line was used for photoluminescence excitation.

3. Experimental results and discussion

3.1. Raman results

The chalcopyrite crystal $A^IB^{III}C_2^{VI}$, with space group $I\bar{4}2d$, has eight atoms per primitive cell. $CuGa_5Se_8$ crystallizes in a chalcopyrite-related structure. To our knowledge, the space group of $CuGa_5Se_8$ has not yet been published. Marin et al. [6] made an assumption that $CuGa_5Se_8$ crystallizes in space group $P\bar{4}2m$ like $AgIn_5Se_8$. The unit cell parameters of $CuGa_5Se_8$ are very close to the unit cell parameters of $CuGaSe_2$. So it is expected that its vibrational spectra is very similar to the chalcopyrite one. Its vibrational spectrum consists of 24 zone-center vibrational modes:

$$1A_1 + 2A_2 + 3B_1 + 4B_2 + 7E,$$

where the E-modes are doubly degenerated. These modes are classified into three acoustic ($B_2 + E$) and 21 optical modes ($1A_1 + 2A_2 + 3B_1 + 3B_2 + 6E$). Except for two silent modes ($2A_2$), there are 22 Raman active modes:

$$1A_1 + 3B_1 + 3B_2(LO) + 3B_2(TO) + 6E(LO) + 6E(TO).$$

Correct assignment of the lattice vibrations is of great importance for a fundamental understanding of the structural properties of chalcopyrites. However, this is not always an easy task, because of the difficulties in growing high quality bulk crystals, the great variety of defects in the chalcopyrite materials and its dependence on a deviation from stoichiometry.

The Raman spectrum of the MOCVD grown $CuGa_5Se_8$ layer with the fitting result are shown in Fig. 1. The Bridgman grown $CuGa_5Se_8$ single crystal showed very

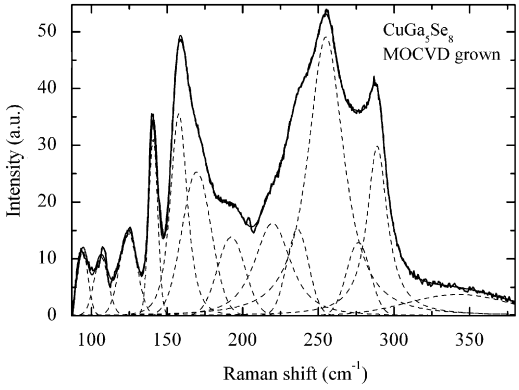

Fig. 1. The room-temperature Raman spectra of MOCVD grown $CuGa_5Se_8$ polycrystalline layer and the result of fitting. Twelve peaks were detected from the spectra. The peak at 93 cm^{-1} is due to the cut-off of the filter and is not taken into account.

similar spectrum. Because of the slightly asymmetric shape of Raman peaks, each peak was fitted using Pearson VII function [12]. Twelve peaks were detected from these spectra. For comparison, Raman peak positions and possible mode assignments, as discussed in the following are listed in Table 1. It is seen from the table, that the A_1 peak at 161 cm^{-1} of a $CuGa_5Se_8$ single crystal is shifted to higher wavenumbers by 3 cm^{-1} compared to the A_1 peak position at 158 cm^{-1} of a $CuGa_5Se_8$ polycrystalline thin film. Negative and positive shifts attributed to the stress in the polycrystalline films can also be observed for other Raman modes.

According to the simplified version of Keating's model, the frequency of the A_1 mode v that results from the motion of the Se atom with the cations remaining at rest, is given by [13]

$$v \approx \sqrt{\frac{k}{M_{Se}}}, \tag{1}$$

where k is a force constant related to the cations–anion bond-stretching forces and M_{Se} is the mass of the Se atom. The vacancies present in OVCs tend to reduce the stretching forces, and thereby the corresponding vibrational frequencies. Since in first approximation the vibrational frequencies in chalcopyrites depend mainly on the interaction of the nearest neighbor atoms and taking also into account that only one vacancy exists for each four Se atoms in the OVC [1], it can be assumed that for the A_1 mode k is reduced by 25% as compared to its value in the normal chalcopyrite. Under this assumption, we can calculate the approximate value of the A_1 mode frequency v' of $CuGa_5Se_8$:

$$v' \approx \sqrt{\frac{0.75k}{M_{Se}}} \approx 0.87v, \tag{2}$$

where v is the A_1 mode frequency in $CuGaSe_2$. The frequency of the A_1 mode for $CuGaSe_2$ at room temperature is 184 cm^{-1} [14], giving us the frequency of 161 cm^{-1} for the A_1 mode in $CuGa_5Se_8$. The observed Raman peaks at 161 and 158 cm^{-1} of a $CuGa_5Se_8$ single crystal and polycrystalline thin film, respectively, are in very good agreement with the theoretically expected value. The A_1 Raman mode of $CuGa_5Se_8$ at 160 cm^{-1} was also observed in Ref. [7].

The B_1 modes involve the motion of the cations. Since the presence of ordered vacancies on Se sites is not expected to occur in these materials, the frequencies of these modes in OVC are expected to be very similar to that observed in $CuGaSe_2$ [15]. Thus, the mode at 117 and 124 cm^{-1} in $CuGa_5Se_8$ single crystal and polycrystalline thin film, respectively, probably corresponds to the second-lowest frequency B_1 mode reported at 116 cm^{-1} in $CuGaSe_2$ at 300 K [14]. The lowest frequency B_1 mode, whose corresponding values in $CuGaSe_2$ and $CuGa_3Se_5$ are 76 and 72 cm^{-1} [16,17], respectively, is not observed in our spectrum due to the limitations of our experimental system. The highest frequency B_1 mode, which should be very weak because it corresponds to the motion of the cations in antiphase, is expected to be observed close to the A_1 peak. This mode has not yet been reported in $CuGa_3Se_5$ or $CuGa_5Se_8$ even at low temperatures.

The remaining modes should be assigned as B_2 and E modes that mostly correspond to the combined motion of all the atoms. Hence, by similar considerations given for the A_1 mode, it is expected that its frequencies are slightly lower than those observed in $CuGaSe_2$ [15]. Thus the peaks at around 255, 236, 220 and 192 cm^{-1} in polycrystalline $CuGa_5Se_8$ and at 253, 235, 216 and 186 cm^{-1} in a $CuGa_5Se_8$ single crystal, can be related to 273, 261, 239 and 199 cm^{-1} in $CuGaSe_2$, respectively. The calculated

Table 1
Raman peak positions, obtained form the fitting, and possible mode assignments

Raman peak position (cm^{-1})					
MOCVD grown $CuGa_5Se_8$	Bridgman grown $CuGa_5Se_8$	$CuGaSe_2$, Ref. [14]	$CuGa_3Se_5$, Ref. [17]	$CuGa_5Se_8$, Ref. [7]	Possible origin
343	344	–	–	–	B_2+E
289	293	–	286	289	B_2+E
277	280	–	274	–	B_2
255	253	273	252	259	E
236	235	261	–	–	B_2 or E
220	216	239	220	–	E
–	–	–	200	–	E
192	186	199	187	–	B_2
170	168	–	–	–	B_2+E
158	161	184	166	160	A_1
141	142	–	142	–	E
124	117	116	–	–	B_1
106	99	96	105	107	E
–	–	–	90	93	B_1
–	–	–	72	78	B_1
–	–	60	64	–	B_2
–	–	–	48	–	E

ratio of each pair of corresponding frequencies in $CuGa_5Se_8$ and $CuGaSe_2$ ν'/ν varies from 0.90 to 0.94 which as also found for $CuGa_3Se_5$ Raman peaks in Ref. [15]. The peak at 141 cm^{-1} probably corresponds to E mode, reported at 142 cm^{-1} in $CuGa_3Se_5$ [17]. The peak around 289 cm^{-1} in $CuGa_5Se_8$ probably corresponds to a combination of the lowest-energy B_2 mode, which is expected to occur at around 53 cm^{-1}, and the E mode at 236 cm^{-1}. Similarly, the peak around 170 cm^{-1} in $CuGa_5Se_8$ probably corresponds to a combination of B and the E modes. Such combinations have also been observed in $CuGaSe_2$ and $CuGa_3Se_5$ [14,15].

We also observed the broadening of Raman peaks in $CuGa_5Se_8$ compared to $CuGaSe_2$. It is expected that high concentration of defects in OVCs leads to the formation of concentration fluctuations [7]. Such spatially extended effects caused by mixed defects and clusters can decrease the phonon lifetimes, which may be responsible for the broadening of Raman bands. This can be taken as an indication of a reduction in crystalline quality due to a large density of defects in $CuGa_5Se_8$.

3.2. Photoluminescence results

Only one broad asymmetric band at 1.788 and 1.765 eV was observed at 10 K in the PL spectra of Bridgman grown $CuGa_5Se_8$ single crystal and MOCVD grown polycrystalline layer, respectively (Fig. 2). PL band positions are at much lower energies compared to the bandgap energy of $CuGa_5Se_8$ ($E_g = 1.811$ eV at 300 K and $E_g(0) \approx 1.917$ eV [6]). Similar spectrum was obtained for $CuGa_3Se_5$ [18]. The asymmetric shape and the position of the PL band suggest that there are Coulomb potential fluctuations induced due to the random distribution of unscreened charged defects present in our samples. These potential fluctuations will lead to a local perturbation of the band structure, thus broadening the defect level distribution and forming band tails [18,19]. Radiative recombination in such crystals is

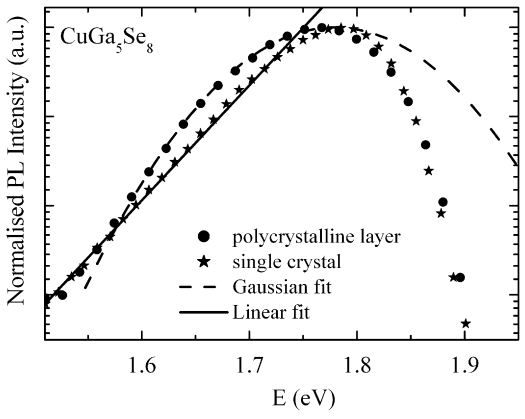

Fig. 2. Normalized PL spectra of polycrystalline and single crystal $CuGa_5Se_8$ at 10 K. The lines represent the fittings of the low-energy side of the PL bands. The polycrystalline and single crystal $CuGa_5Se_8$ showed Gaussian and exponential spectral dependence of the low-energy tail of emission, respectively.

therefore governed by the recombination of carriers localized in spatially separated potential wells originating from Coulomb potential fluctuations. The analysis of the PL data suggests that the emission is due to band-to-tail (BT) or band-to-impurity (BI) recombination, because both emissions show very similar behavior [20].

Siebentritt et al. [21] have analyzed the shape of the band tails in case of fluctuating potentials using two different models. According to them, the low-energy tail of PL emissions can be described by a Gaussian or an exponential spectral dependence. This based on the more general theoretical analysis of the density of states function by Osipov and Levanyuk [22]. The low-energy sides of the PL band of the $CuGa_5Se_8$ samples analyzed in the present paper showed Gaussian shape and exponential decay for the polycrystal and single crystal, respectively. It is an indication of the presence of deeper fluctuations with the Gaussian shape density of states function in polycrystal while the density of states function in the band tails of a single crystal has an exponential distribution. Deeper potential fluctuations in $CuGa_5Se_8$ polycrystal also explain the shift of the PL band position towards lower energies compared to the single crystal. Like in Ref. [21], the average amplitudes of the fluctuations $\gamma = 62$ and 113 meV for the $CuGa_5Se_8$ single crystal and polycrystal, respectively, were determined from the exponential and Gaussian spectral dependencies, respectively [22]:

$$I(E) \sim \exp\left(-\frac{E}{\gamma}\right) \quad \text{or} \quad I(E) \sim \exp\left(-\frac{(E-E_0)^2}{2\gamma^2}\right), \tag{3}$$

where E_0 is assumed to represent an average emission energy in the case of fluctuating potentials.

Excitation power and temperature dependent (Figs. 3 and 4) photoluminescence measurements indicate that our spectra are dominated by the BT-type recombination that involves free electron and a hole that is localized in the valence band tail [22]. Although other models can be used, we follow in our discussion here the arguments and the nomenclature used there. Due to their small effective mass, almost all electrons are free. Holes are localized in the valence band potential wells and form so-called pseudo-acceptor states. The activation energy of the thermal quenching of the PL band allows us to evaluate the average depth of these pseudo-acceptor states. From Arrhenius plot of thermal quenching of the PL band (Fig. 3), we obtained an estimation of thermal activation energy of pseudo-acceptor states 40 ± 8 and 168 ± 5 meV for single crystal and polycrystalline $CuGa_5Se_8$, respectively. The $ln\, I(T)$ versus $1000/T$ dependence was fitted with theoretical expression for discrete energy levels proposed in [23]

$$\Phi(T) = \frac{\Phi_0}{1 + \alpha_1 T^{3/2} + \alpha_2 T^{3/2} \exp(-E_T/kT)}, \tag{4}$$

where Φ is integrated intensity, α_1 and α_2 are the process rate parameters and E_T is the thermal activation energy. Despite the similarity between the experimental and theoretical dependencies, it is clear that in the case of BT

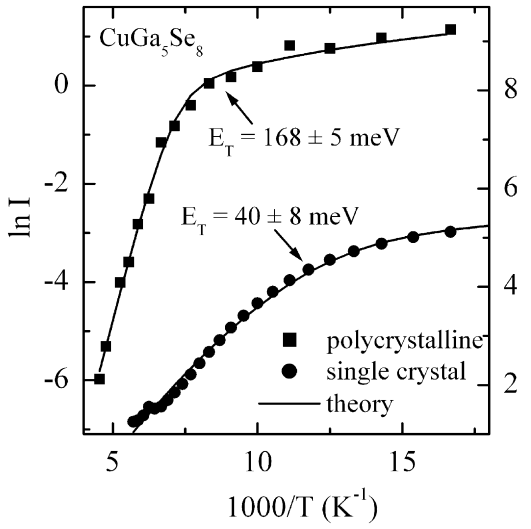

Fig. 3. Arrhenius graph of $CuGa_5Se_8$ single crystal and polycrystalline layer obtained from the temperature dependence of the PL spectra. Solid lines represent the fitting of the experimental data with the theoretical expression (4). Thermal activation energies of 168 and 40 meV were obtained for polycrystalline and single crystal $CuGa_5Se_8$, respectively.

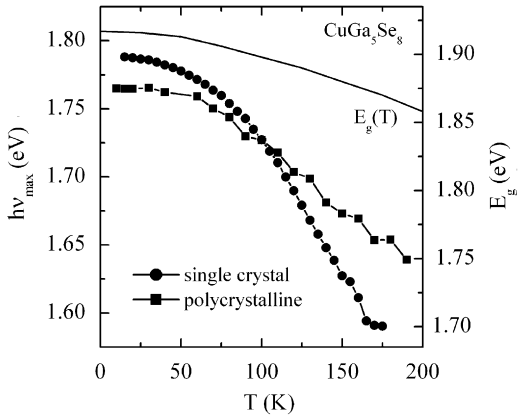

Fig. 4. Temperature dependence of the PL band peak position. Solid line represents the temperature dependence of the bandgap energy E_g of $CuGa_5Se_8$ [6].

type recombination, the fitting is not completely valid due to continuous tail states.

Higher thermal activation energy in $CuGa_5Se_8$ polycrystalline film is probably related to the coexistence of BT- and BI-type recombination in the sample, the latter being related to a deeper acceptor level. The Gaussian shape of the low-energy tail of PL emission supports this idea.

In Fig. 4 the temperature dependence of the PL band peak position along with the bandgap energy E_g of $CuGa_5Se_8$ [6] is shown. The peak position energy decreasing rate exceeds the bandgap energy decreasing rate with temperature. This feature is predicted by the theory of heavily doped semiconductors [22] and was also observed in $CuGa_3Se_5$ [18]. More detailed analysis of the temperature dependence of PL band position in case of heavily doped materials can be found in Refs. [19,20].

From the excitation power dependence, the blue shift of the PL band with the magnitude of about 15 and 23 meV per decade for $CuGa_5Se_8$ single crystal and polycrystalline layer, respectively, was detected. This again confirms that the observed emission results from BT or BI recombination [22]. The observed shift is larger for the sample with deeper potential fluctuations, as predicted by the theory.

4. Conclusions

The Raman and PL properties of the ordered vacancy compound $CuGa_5Se_8$ have been studied. Twelve peaks were detected from the room-temperature Raman spectra with the A_1 mode around 160 cm^{-1}. One broad asymmetric PL band at 1.788 and 1.765 eV was observed at 10 K in the PL spectra of $CuGa_5Se_8$ single crystal and polycrystalline layer, respectively. The analyses of the PL data suggest that the emission is due to BT- or BI-type recombination, indicating the presence of potential fluctuations due to high concentration of charged defects.

Acknowledgments

This work was supported by INTAS Grant no. 03-51-6314 and by the Estonian Science Foundation Grant G-6554.

References

[1] S.B. Zhang, S.H. Wei, A. Zunger, H. Katayama-Yoshida, Phys. Rev. B 57 (1998) 9642.
[2] M.A. Contreras, B. Egaas, K. Ramanathan, J. Hiltner, A. Swartzlander, F. Hasoon, R. Noufi, Proc. Photovoltaic Res. Appl. 7 (1999) 311.
[3] D. Schmid, M. Ruckh, F. Grunwald, H.W. Schock, J. Appl. Phys. 73 (1993) 2902.
[4] S.H. Wei, S.B. Zhang, A. Zunger, Appl. Phys. Lett. 72 (1998) 3199.
[5] G. Marin, S.M. Wasim, C. Rincon, G. Sanchez Perez, P. Bocaranda, I. Molina, R. Guevara, J.M. Delgado, Appl. Phys. 95 (2004) 8280.
[6] G. Marin, J.M. Delgado, S.M. Wasim, C. Rincon, G. Sanchez Perez, A.E. Mora, P. Bocaranda, J.A. Henao, J. Appl. Phys. 87 (2000) 7814.
[7] C.-M. Xu, W.-H. Huang, J. Xu, X.-J. Yang, J. Zuo, X.-L. Xu, H.-T. Liu, J. Phys. Condens. Matter 16 (2004) 4149.
[8] N.S. Orlova, I.V. Bodnar, T.L. Kushner, Cryst. Res. Technol. 38 (2003) 125.
[9] N.S. Orlova, I.V. Bodnar, T.L. Kushner, J. Phys. Chem. Solids 64 (2003) 1895.
[10] M. Leon, R. Serna, S. Levcenko, A. Nateprov, A. Nicorici, J.M. Merino, E. Arushanov, Phys. Stat. Sol (A) 203 (2006) 2913.
[11] A. Bauknecht, S. Siebentritt, J. Albert, M.C. Lux-Steiner, J. Appl. Phys. 89 (2001) 4391.
[12] E.P. Petrov, J. Quant. Spectrosc. Radiat. Transfer 103 (2007) 272.
[13] H. Neumann, Helv. Phys. Acta 58 (1985) 337.
[14] F.J. Ramirez, C. Rincon, Solid State Commun. 84 (1992) 551.
[15] C. Rincon, S.M. Wasim, G. Marin, J.M. Delgado, J.R. Huntzinger, A. Zwick, J. Galibert, Appl. Phys. Lett. 73 (1998) 441.
[16] J. Gonzalez, J.C. Chervin, Jpn. J. Appl. Phys. 32 (Suppl.) (1993) 575.
[17] C. Rincon, S.M. Wasim, G. Marin, E. Hernandez, G. Sanchez Perez, J. Galibert, J. Appl. Phys. 87 (2000) 2293.
[18] M. Grossberg, J. Krustok, A. Jagomägi, M. Leon, E. Arushanov, A. Nateprov, I. Bodnar, Thin Solid Films 515 (2007) 6204.

[19] J. Krustok, H. Collan, M. Yakushev, K. Hjelt, Phys. Scripta (T) 79 (1999) 179.
[20] A. Jagomägi, J. Krustok, J. Raudoja, M. Grossberg, M. Danilson, M. Yakushev, Physica B 337 (2003) 369.
[21] S. Siebentritt, N. Papathanasiou, M.Ch. Lux-Steiner, Physica B 376–377 (2006) 831.
[22] A.P. Levanyuk, V.V. Osipov, Sov. Phys. Usp. 24 (1981) 187.
[23] J. Krustok, H. Collan, K. Hjelt, J. Appl. Phys. 81 (1997) 1442.